



# Partial discharge measurements and life estimation in DC electrical insulation during voltage transients and steady state

R. Ghosh<sup>a,b,\*</sup>, P. Seri<sup>b</sup>, G.C. Montanari<sup>a,b</sup>

<sup>a</sup> Centre for Advanced Power Systems, Florida State University, Tallahassee, USA

<sup>b</sup> Department of Electrical, Electronic and Information Engineering, University of Bologna, Italy

## ARTICLE INFO

### Keywords:

HVDC insulation  
Insulation life  
Insulation testing  
Partial discharges  
Life estimation  
Reliability  
Asset management

## ABSTRACT

The design and operation of DC insulation systems is more complex than for AC sinusoidal supply. The most subtle issues are how the electric field in DC can vary with operation and affect the partial discharge inception voltage and partial discharge phenomenology. During operation, a DC insulation system is indeed subjected to voltage and load transients, the former due to energization and voltage polarity inversion. This paper sheds some lights on such issues, going through another fundamental problem, that is, how to carry out effective partial discharge detection under DC supply, both in steady state and during voltage transients. An algorithm that can enable automatic and unsupervised partial discharge measurements in DC electrical apparatus is presented and validated based on partial discharge monitoring performed on test objects representing defective insulation systems. Identification of the source generating partial discharges, which is the basis for diagnostic and condition maintenance, is achieved without the support of experts. The impact of voltage transients on the life and reliability of DC insulation systems is modelled in the presence and absence of partial discharges. It is shown that, depending on the repetition rate, the presence of partial discharges, even if only during voltage transients, can dramatically affect the insulation life and cause premature insulation breakdown.

## 1. Introduction

While the use of DC supplies in MV and HV applications is growing impetuously, for applications ranging from energy generation and transmission to distribution and utilization (e.g. in electrified transport), there is still a lack of knowledge on fundamental DC-insulation aging mechanisms and of techniques to measure and monitor the most harmful diagnostic properties, as partial discharges, PD [1, 2]. There is not clear understanding, either, of the phenomenology of PD, under DC supply, for what it concerns both steady state conditions and voltage transients. Actually, DC insulation can be subjected to numerous, repetitive voltage transients during operation life, as those consisting of energization or polarity inversion [3].

During any time-variation of peak or rms voltage, the electric field profile in insulation is governed by the ratio between permittivity and conductivity, while it is conductivity to rule electric field distribution under DC steady state [4–6]. In particular, the field will be driven mostly by permittivity, as in AC, at the beginning of each field transient. This means that during voltage polarity inversions, an electric field large enough to incept PD, which would not be present under steady-state DC,

may exist in insulation defects (cavities, interfaces). In other terms, the partial discharge inception voltage, *PDIV*, can be lower in AC than in DC (depending on operating load/temperature), so that small or no PD activity can occur under steady-state DC for an insulation system, while significant amount of PD can be incepted during voltage transients [7].

There is no doubt, then, that factory quality control, commissioning and operation require PD testing and monitoring technologies that are effective in rejecting noise and identifying PD and their source, both under DC and AC power supply. Those, at present, are partially available only for AC supply [8]–[10]. In addition, developing life models that associate operating life not only to steady-state DC conditions, but also to the accelerated aging effect of voltage transients, is fundamental to reach the objective to design and install insulations systems (e.g. cables) able to deliver the specified life and reliability in correspondence of an expected mean rate of voltage transients.

Eventually, a last but also fundamental issue to be faced is the need of effective methods to perform PD measurements, reject noise and identify PD source typology under DC supply that do not require necessarily the support of experts, which involves often unsustainable costs and delays in insulation condition evaluation.

\* Corresponding author at: Centre for Advanced Power Systems, Florida State University, Tallahassee, USA.

E-mail address: [riddhi.ghosh@unibo.it](mailto:riddhi.ghosh@unibo.it) (R. Ghosh).

<https://doi.org/10.1016/j.epsr.2021.107117>

Received 25 June 2020; Received in revised form 6 February 2021; Accepted 19 February 2021

Available online 27 February 2021

0378-7796/© 2021 Elsevier B.V. All rights reserved.

This paper makes use of an innovative, unsupervised approach to the separation of PD and noise which can work under steady-state DC and under voltage transients, providing automatic separation and recognition of PD and noise, as well as identification of PD-source typology, to infer PD data coming from measurements performed on defective insulation systems during both steady state DC and transient voltage [3, 11]. Electric field behavior under DC steady state and voltage transients and its impact on PD inception voltage is described in Section 2, while the automatic procedure for PD identification and noise rejection is summarized in Section 3. Sections 4 and 5 present and discuss experimental data from PD monitoring of multi-layer polypropylene specimens having the middle layer punched to reproduce a cavity which is able to ignite PD both under AC and DC (at different voltage levels), thus validating the algorithm of Section 2. Eventually, a model able to describe insulation life where PD can be present or absent during DC steady-state operation, and having PD that can be incept at each voltage transients, is derived in Section 6. The model allows correlation between allowable rate of voltage transients and specified life to be established.

## 2. Voltage and field transients in insulation

In steady state DC the electric field profile in an insulated cable is driven by admittance, thus conductivity. However, when instantaneous voltage varies with time, as during energization or voltage polarity inversion, the electric field depends on capacitance, thus permittivity, as in AC. Because of the large dependence of conductivity on temperature, [12, 13], the electric field in insulation under steady state DC can be significantly different than during transients, when it behaves as under an AC supply [4, 11]. An example is shown in Fig. 1, which reports the time variation of electric field magnitude in a flat insulation specimen, 1.2 mm thick, and in a cylindrical cavity (3 mm of diameter, 0.4 mm of height) embedded in it, after application of a voltage step of 8 kV. The ratio between conductivity in the insulation,  $\gamma_b$ , and in the cavity,  $\gamma_c$ , is  $\frac{\gamma_b}{\gamma_c} = 0.1$ , and the ratio between permittivity is  $\frac{\epsilon_b}{\epsilon_c} = 2$ . The time constant that governs the field transition from the instant at which the voltage transient starts and the steady-state DC condition (which depends on the ratio of dielectric permittivity and conductivity, i.e. [14-17]) is  $\tau \approx 5 \times 10^3$  s, that is, much longer than the voltage transient itself. This time constant is the result of the interaction between the redistribution of the electric field in the dielectric (growing line in Fig. 1) and the cavity (decreasing line in Fig. 1), each characterized by a different time constant  $\tau_i = \frac{\epsilon_i}{\gamma_i}$ , being respectively  $5.9 \cdot 10^4$  s for the dielectric, and  $2.9 \cdot 10^3$  s

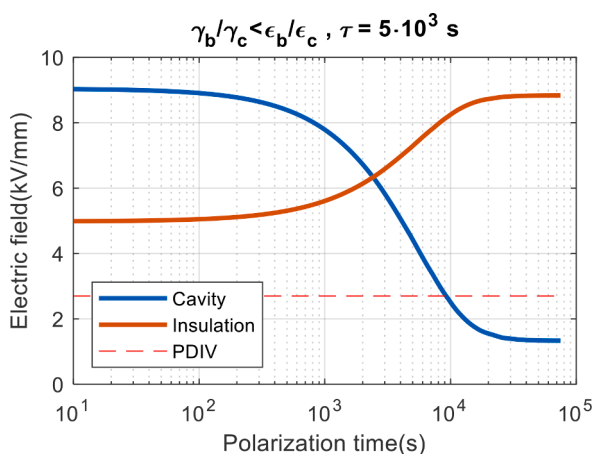


Fig. 1. Field-magnitude time variation in a flat insulation specimen 1.2 mm thick and in a cylindrical cavity (3 mm of diameter, 0.4 mm of height) embedded in it, after application of a voltage step of 8 kV. Isothermal conditions. The partial discharge inception field, estimated according to [18], is indicated.

for the cavity (being  $i$  related to cavity or dielectrics characteristics).

The higher the dielectric conductivity, the shorter the transient time, so that e.g. the same insulation system simulated in eq. (1) can provide  $\tau < 10^3$  s under full load, due to the dependence on temperature of conductivity.

The different parameters driving the electric field profile in DC and AC are also significantly influencing the partial discharge inception voltage,  $PDIV$ . Fig. 1 indicates the value of electric field at which PD inception occurs according to the deterministic expression proposed in [18]. According to the approximate model presented in [19], the ratio between the partial discharge inception voltage in DC and AC,  $PDIV_{DC}$  and  $PDIV_{AC}$ , is given by:

$$\frac{PDIV_{DC}}{PDIV_{AC}} = \frac{|Z_c(\omega)|}{|Z_b(\omega)| + |Z_c(\omega)|} \cdot \frac{R_b + R_c}{R_c} \quad (1)$$

where  $Z$  and  $R$  are the impedance and the resistance representing the capacitive and resistive characteristics of the cavity (suffix  $c$ ) and the insulation (suffix  $b$ ) in their lumped element model ( $abc$  circuit) [1, 19]. For typical values of HV and MV insulating dielectrics,  $PDIV_{DC}$  can be much higher than  $PDIV_{AC}$ , but the opposite can occur under full load if the dependence of conductivity on temperature (coefficient  $\alpha$  [1, 12, 15]) is significant. This is shown in Fig. 2, where the ratio of  $PDIV_{DC}$  to  $PDIV_{AC}$  is expressed as function of temperature, for three values of the coefficient,  $\alpha$ , for a specific defect size ( $h_c=0.4$  mm). Conductivity at 0°C for the insulation is  $1.72 \times 10^{-15}$  S/m, with relative permittivity of 2.1, while the conductivity for the cavity medium (air) is  $10^{-15}$  S/m, with relative permittivity of 1. Therefore, there can be cases when the DC steady state operation may be affected by PD or not depending on load, and, in addition, electric field transients can generate PD, as shown in [20]. These PD will extinguish or continue, even if at a much lower repetition rate [14, 15, 21], when  $t$  approaches  $\tau$ , the electric field transient constant.

Variation of the electric field profile (thus maximum electric field value) and  $PDIV$  in DC steady state with load, as well as the move from  $PDIV_{DC}$  to  $PDIV_{AC}$  during voltage transients, make design of DC insulation extremely complex and, therefore, require, even more than for AC insulation, monitoring of partial discharges during operation life. This is the topic of the next sections.

## 3. Automatic PD identification and noise rejection

Separation of PD from noise and of one source of PD from another, and recognition of recorded signals as belonging to PD or noise is the basis to pursue the goal of identification of the type of source generating

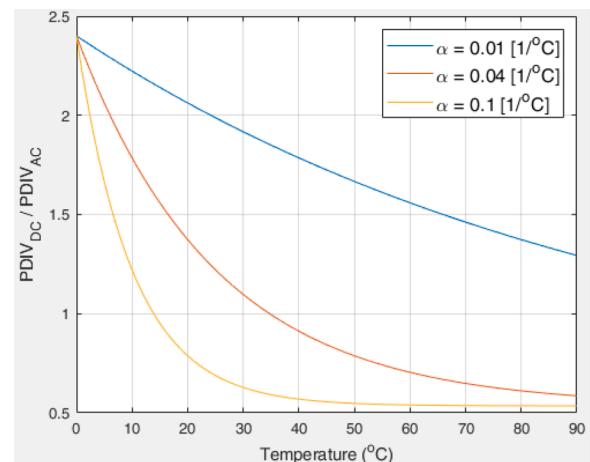


Fig. 2. Ratio of  $PDIV_{DC}$  to  $PDIV_{AC}$  as function of temperature, for three values of the coefficient,  $\alpha$ , expressing the dependence of conductivity on temperature, for a specific defect size ( $h_c = 0.4$  mm).

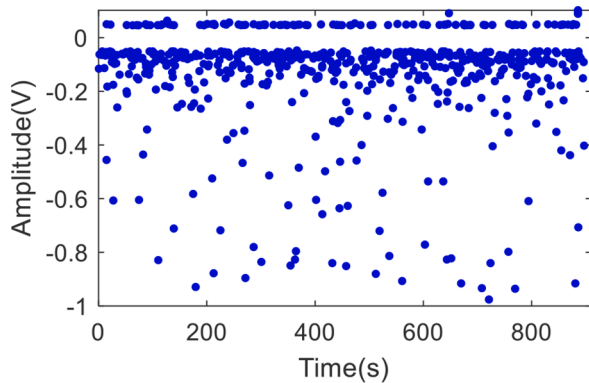
PD. Identification is crucial, on the other hand, to carry out diagnostics and condition-based maintenance (CBM) procedures, including health index and residual life estimation [16, 21].

The other crucial aspect is that PD inference should be carried out automatically, without the supervision of experts that may cause unacceptable increase of response times and costs.

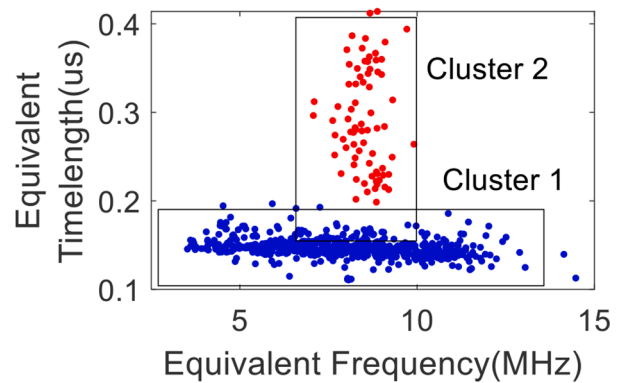
The application of an automatic and unsupervised algorithm for separation, recognition and identification, which can be applied successfully to handle PD data from testing DC insulation systems in typical operation conditions, where frequent energization and voltage polarity inversion break steady state behavior, is shown in the following.

### 3.1. Separation

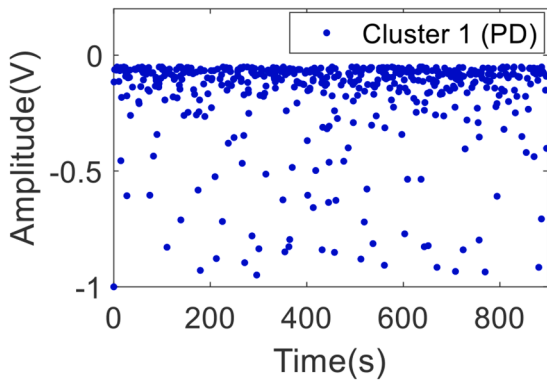
For the separation of clusters, multiple parameters were extracted from each signal and series of signals recorded during PD measurements, using signal features such as equivalent time length, equivalent frequency, entropy of each signal, as well as kurtosis and skewness of the magnitude distribution. Using multiple parameters increases the possibility of identifying characteristics that can provide good discrimination between groups of signals belonging to different sources. The use of an appropriate dimensionality reduction technique can then allow to view the projection of the high dimensional data into a two-dimensional subspace. This, as well as the removal of redundant features, can be achieved through Principal Component Analysis (PCA). Hierarchical clustering is used for automatically clustering the data. The details of the technique can be found in [11, 22].



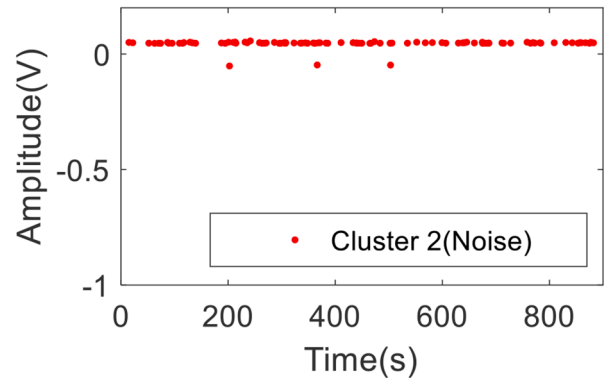
(a)



(b)



(c)



(d)

Figure 3 shows, as an example, a PD pattern from measurements performed on a MV cable with an artificial defect. Two clusters exist in the projection of the multi-dimensional clustering map into an equivalent two-dimensional Principal Component Plane ( $PC1$  vs  $PC2$ ). Clusters are separated by the automatic clustering algorithm in Fig. 3(b), and the sub-patterns of the original global pattern, Fig. 3(a), are reported as extracted from clusters, Fig. 3(c) and 3(d). Recognition of the type of signals belonging to each cluster (indicated in the figure) is performed as follows.

### 3.2. Recognition

Statistical tests, as those mentioned e.g. in [6], can be performed on PD amplitude and repetition rate distributions relevant to each sub-pattern in order to recognize those patterns related to noise to those due to PD.

These tests include fitting to the two-parameter Weibull distribution of PD-pulse magnitude,  $q$ , that is [23]:

$$F(s) = 1 - e^{-\left(\frac{q}{\alpha}\right)^\beta} \quad (2)$$

where  $\alpha$  is the scale parameter (corresponding to charge value at probability 63.2%) and  $\beta$  the shape parameter. The Weibull distribution has been proved to fit well to PD amplitude values, being an extreme-value statistics (as insulation breakdown voltage), but it has not any reason to hold also for noise. Note that charge amplitude in (2) can be replaced by any other means used to measure PD, such as pulse voltage

Fig. 3. Example of separation from PD tests performed on a MV cable with an artificial defect. Global time-resolved PD pattern, Fig. 3(a), principal component 2-dimensional map (Fig. 3(b)), where two clusters are extracted and separated automatically. The sub-patterns of the original global pattern as derived by Clusters 1 and 2 are reported in Figs. 3(c) and 3(d).

magnitude. Note also the eq. (2) holds for any type of supply voltage waveform, likely with slightly different values of the shape parameters (see later).

Other statistical tests can be applied to the pulse shape, because PD signals are inherently more structured compared to noise signals, the latter being mostly random and, thus, lacking of a well-defined structure. This can be quantified e.g. using a linear prediction (LP) analysis which gives an estimate for the representation of the measurement circuit response, while the error (called the LP residual) between the actual signal and predicted signal is the excitation signal (discharge) [22]. Referring to clusters 1 and 2 of Fig. 3, Figs. 4a and 4b show an example of typical PD and noise signals, respectively, along with residuals and their magnitude probability density distributions. As can be seen, the residual of the PD signal (Cluster 1) is highly skewed (-2.6), while the residual of noise (Cluster 2) has very low skewness (0.3). The isolated peak point of the PD pulse, marked with the arrow in the bottom figure of Fig. 4a, shows why skewness is high for Cluster 1. The amount of skewness can be considered, therefore, a marker for PD and noise recognition within the clusters separated as in A.

### 3.3. Identification of PD source typology

Fig. 3 and Fig. 4 provide an example of how the algorithm can work properly for automatic cluster separation, being the basis to recognize PD and reject noise, for a case of DC-steady state voltage supply. Indeed,

Fig. 3 reports the case of separation and automatic clustering, which shows two clusters of data that were recognized (automatically), also by the algorithm of Fig. 4, as belonging to PD and noise.

However, a further step is needed, that is, identification of the type of source generating PD. As mentioned, this is a fundamental tool to achieve effective diagnostics, condition assessment and maintenance.

Different methodologies can be applied for this purpose, [12, 16]. Various markers can support a fuzzy-logic based approach, as shown in [10], according to which PD can be primarily identified as belonging to three categories with decreasing harmfulness, that is, internal, surface and corona discharges.

One of the markers is the shape parameter of the Weibull distribution of PD-pulse charge magnitude, eq. (2). Previous experience had shown that shape parameter values for PD generated in cavities embedded in insulation or at interfaces (internal discharges), which is the type of defect considered here, range between 1.5 and 5 in AC. In DC, the expected values of  $\beta$  are larger than in AC, often ranging between 2 and 10. Surface discharges provide lower values of  $\beta$ , while corona discharge amplitudes are less dispersed, thus  $\beta$  is higher (see [6]).

As an example, Fig. 5 reports Weibull plots of charge amplitude for the same clusters, 1 and 2, of Fig. 4. As can be seen, the values of the shape parameters are 2.2 and 15.2, respectively, but the quality of fitting, measured by the  $R^2$  goodness of fit test, is 0.88 for PD and 0.5 for noise. This confirms that Cluster 2 (bad fitting to (2)) and an abnormal value of  $\beta$  is populated by noise signals, while Cluster 1 contains actual

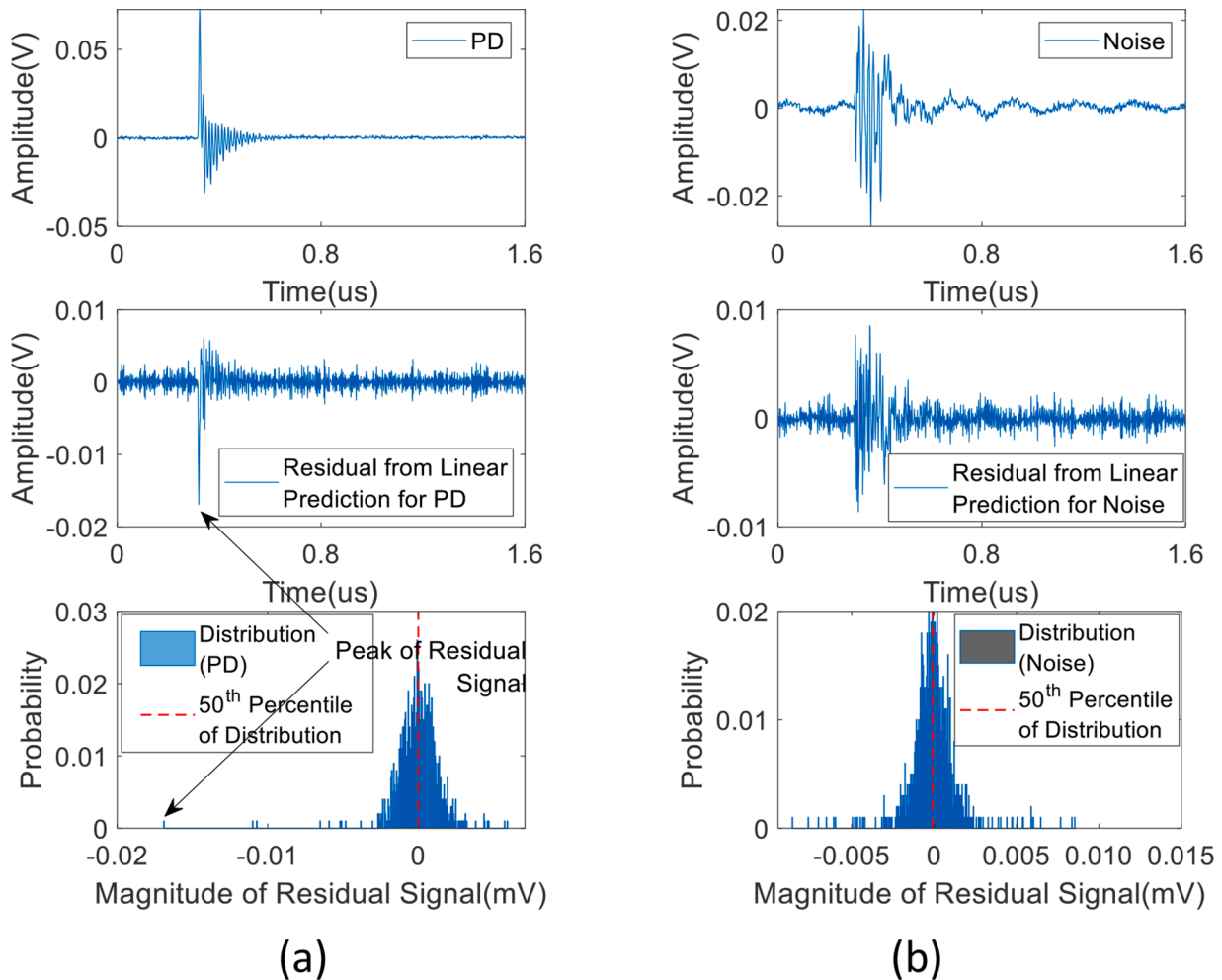


Fig. 4. Recognition of PD and noise pulses through statistical pulse shape processing: Linear Prediction residual of signals representing (a) PD (cluster 1) and (b) noise (cluster 2) pulse amplitudes for an internal discharge on a multilayer specimen. Above: signal, middle: residual from LP, below: probability distribution of the residual.

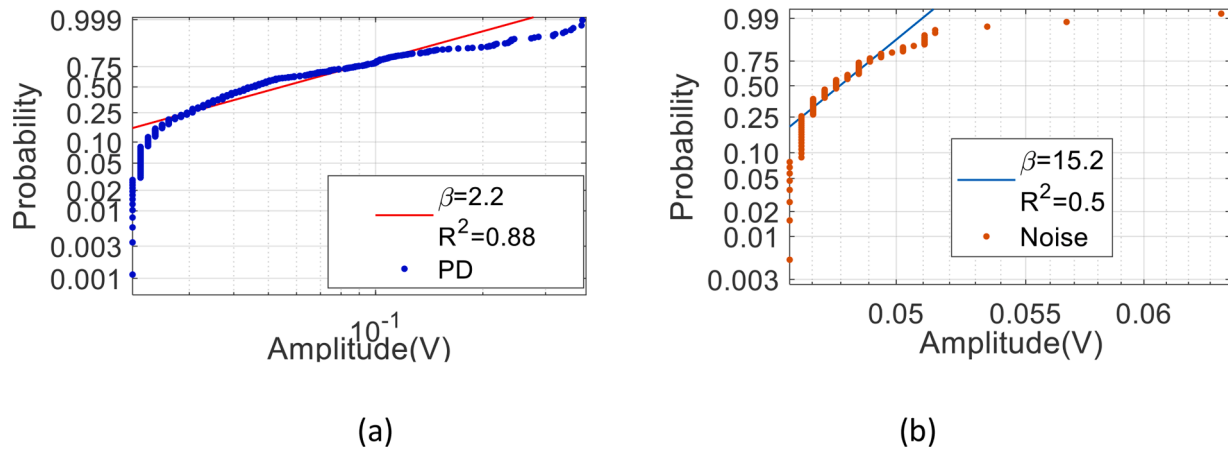


Fig. 5. Weibull plots of charge amplitude for Clusters 1 (a) and 2 (b), of Fig. 4. The values of the shape parameters ( $\beta$ ) and goodness-of-fit ( $R^2$ ) are reported

PD pulses which, based on the shape parameter value, are generated by internal discharges.

#### 4. Application to experimental results

DC PD tests were carried out on objects made of three or more layers of polymeric insulation (polypropylene), having the middle layer punctured to simulate an internal cavity where PD can incept, depending on cavity size, applied voltage and temperature and dielectric characteristics of the polymeric material layers. PD were monitored during transient and in DC steady-state by an innovative detector having ultra-large bandwidth, which performs what described in Section 3 and uses, for these tests, a high-frequency current transformer (HFCT) sensor. A schematic arrangement for the setup has been shown in Fig. 6. Signal to noise ratio was reasonably high, being tests carried out in the laboratory.

Specimens were energized using a continuously increasing voltage, with mean slew rate of 1 kV/s, and material properties were chosen appropriately so that at room temperature the steady-state DC field was lower or higher than the PD inception field and during voltage transient the  $PDIV_{AC}$  was exceeded largely (which comes from insulating material properties, namely conductivity and permittivity). PD were monitored from time zero to times longer than the electric field transient time characteristic,  $\tau$ .

Fig. 7 shows an example of PD measurement results, obtained after separation based on clustering on a two-dimension map obtained by the Principal Component (PC) analysis (Section 3). In this case, PD occur during electric field transient, but not in steady state. Each point of Fig. 7 was obtained after clustering and separation of PD from noise.

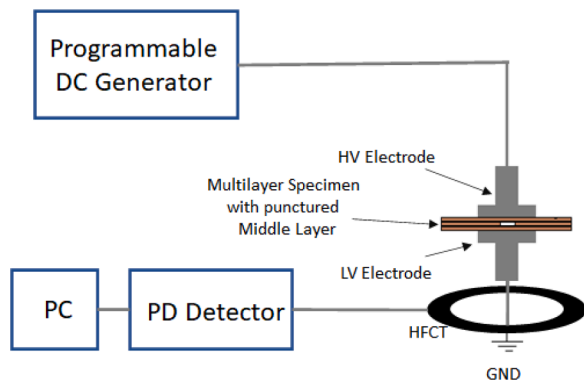


Fig. 6. Experimental setup in the laboratory for measuring PD in a test object made of three layers of polypropylene with the middle layer punctured to simulate an internal cavity, under DC.

Separation is illustrated in Fig. 8 which displays two-dimensional Principal Component plane, with clusters evidenced by circles [3]. Recognition of which set of acquired pulses belongs to noise and which to PD was carried out through the criteria explained above. It is noteworthy that two different types of noise were recognized (like due to a white noise and power electronics emission).

A case where PD occur during both energization transient and in steady state is summarized in Fig. 9, that reports the PD events as a function of time, together with the estimate of the time constant,  $\tau$ . The values of  $PDIV$  in AC and DC (estimated by (1), where each term multiplied by inception field and cavity height represents the relevant  $PDIV$  [19]) are also indicated. As can be seen, PD pulses are mostly occurring during the energization transient, after the voltage exceeds the  $PDIV_{AC}$ , but a significant amount of events is present also while the electric field reaches steady state (being voltage in steady state  $> PDIV_{DC}$ ). Fig. 10 shows clustering and separation for pulses belonging to the PD or to noise, [3]. Once more, clustering separates clearly noise from PD (noise can be rejected, as in the case of Fig. 4), during both transient and steady-state.

Pulse maximum voltage Weibull plots for the PD measurements relevant to Fig. 9, for transient and steady state, and Fig. 7 for transient, are displayed in Fig. 11. As can be seen, fitting to Eq. (2) is reasonably good, and the values of shape parameters are 1.5 and 1.8 for the two cases of transient PD, and 4.2 for steady state condition. These values fit to the range of internal discharges, for AC and DC PD data respectively.

#### 5. Discussions

The results obtained from the procedure of separation, recognition and identification seem to provide interesting clues. We can discuss then a few major focus points, having in mind that all the results reported here are relevant to laboratory testing.

One is that the automatic separation algorithm seems effective in providing at least a couple of principal components where the recorded pulses can be grouped, with a limited extent of cluster overlap that enables the automatic procedure to work without expert supervision. Experts are not needed, also, for recognition of the clusters containing noise or PD pulses, and, eventually, to discern the type of defect(s) which is (are) source(s) of PD. As assessed and shared by most researchers (e.g. [25]), diagnostic is effective in prompting condition-based maintenance if the harmfulness of a PD source, in terms of aging rate, is ascertained. Algorithms for health condition estimation of an electrical apparatus can then be developed, such as automatic and unsupervised information about maintenance time and system reliability [21].

It is noteworthy that separation does not make any difference between transient and steady PD, being all included in the same cluster.

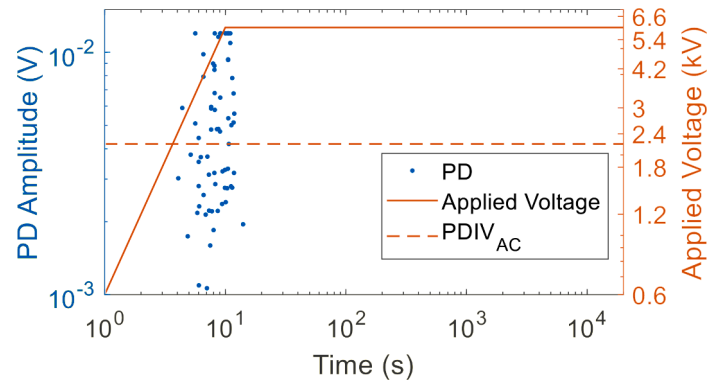


Fig. 7. Applied DC voltage and PD events measured in a three-layer specimen. Rise time 10 s. Room temperature.  $PDIV_{AC}$  is the partial discharge inception voltage in AC. The steady state value of supply voltage is lower than the  $PDIV_{DC}$  (9.2 kV).

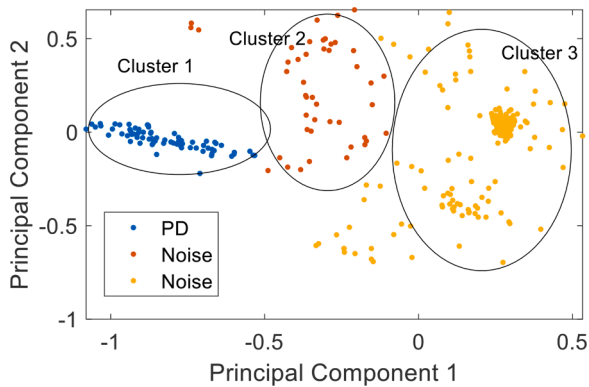


Fig. 8. Example of projection of the multi-dimensional clustering on an equivalent Principal Component Map, related to Fig. 7, with clusters evidenced by circles. Pulses belonging to noise and to PD are indicated.

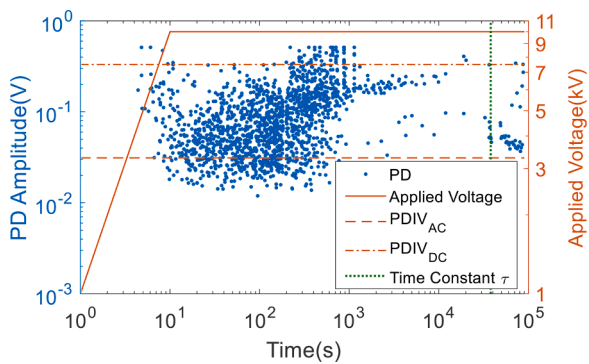


Fig. 9. Example of a case where PD events occur during energization field transient and in DC steady-state. The applied voltage values are reported in the background, together with the estimate of the time constant,  $\tau$ . The values of  $PDIV_{AC}$  and  $PDIV_{DC}$  are also indicated. Same type of specimen as in Fig. 8.

Indeed, separation is based mostly on the pulse shape features, and there is no reason to think that PD pulses during voltage transients should be different from those in steady state DC.

A difference, and this is a second focus point, is in the values of shape parameter of PD-pulse magnitude distribution,  $\beta$ . The shape parameter is sensitive to pulse-magnitude dispersion, and, therefore, to the relation between PD occurrence time, voltage-time variation and statistical delay of the PD-pulse firing electron [2]. As  $\beta$  varies considerably from voltage transients, where it is about 1.5 in the experiments and type of defect presented here, to 4.2 under steady state, for the same defect, this that

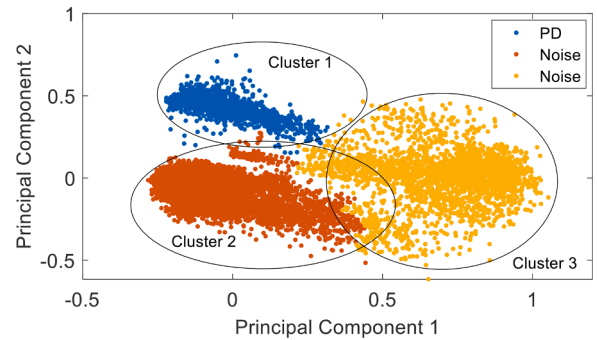


Fig. 10. Example of projection of the multi-dimensional clustering on an equivalent Principal Component Map, related to Fig. 9. Pulses belonging to noise and to PD are indicated.

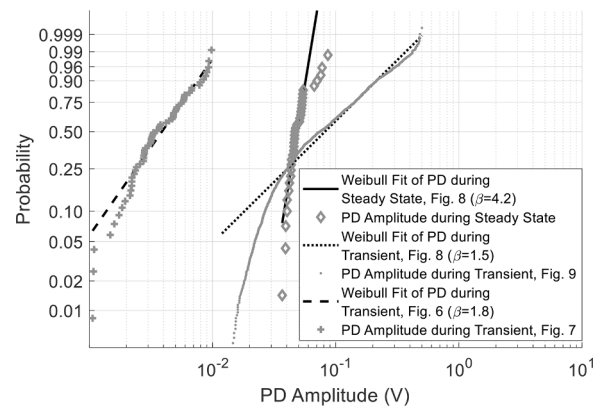


Fig. 11. PD-pulse voltage magnitude values fitted to Weibull plots for PD measurements carried out in transient and steady state DC. Data for transients refer to Fig. 7 and Fig. 9, while those from steady-state DC conditions come from Fig. 9.

can help to discriminate between transient and steady discharges (in addition to PD-pulse repetition rate [19]). In a way, it can be argued that during transient the value of  $\beta$  is typical of internal discharges under AC field [9], while during steady state it fits to DC field PD phenomenology [6] (indeed, features as availability of first electron and memory effect that play a different role in PD phenomenology under DC and AC).

Another interesting observation stems from Fig. 9. During the initial part of the electric field transient, PD pulses have mean repetition rate of 1.5 pulse per second. After  $PDIV_{DC}$  is exceeded, and for time still well lower than the estimated value of  $\tau$ , the mean repetition rate becomes

approximately stable at 0.001 pulse per second. This indicates that most of the accelerated aging effect of PD is developed during the first part of the energization or voltage-polarity inversion transients. Considering that, depending on temperature and for typical materials and defects present in HV polymeric DC cables,  $\tau$  could range anywhere between a few minutes to several minutes. Even if PD occur with high repetition rate only for a fraction of  $\tau$ , it can be argued that the in case of frequent voltage transients, the presence of PD, especially during the first part of the field transient, can be harmful for cable reliability.

Life models have to be developed to account for such a potential source of accelerated aging, providing an estimate of the rate of energizations-inversions that an insulation systems operating under DC supply would withstand to reach the specified life. This is the topic dealt with in the next section.

### 6. Life estimation under repetitive voltage transients

Having earned the capability of recognizing PD and noise, rejecting noise and identifying the type of PD source, in the presence or absence of PD in DC steady state, and depending on voltage transient (energization/polarity inversion) rate, the main question is about the possibility of estimating life as a function of the planned mean inversion rate that an insulation system will have to withstand during operation. This would allow a plan for insulation system utilization and would enable reliable design according to life specifications.

The contribution to aging and breakdown time (life) of an electrical insulation supply by DC voltage with or without PD, and subjected to voltage transients able to trigger PD can be explained resorting to a cumulative aging model (based on superposition effect) as that proposed by Miner in the '40[26]. If, for example,  $t_1$  is the part of life time during which aging occurs under DC steady state and  $t_2$  that corresponding to the mean value of the total time at which PD are active during voltage transients (as energization or voltage polarity inversion), and  $\delta = t_1 / t_2$ , aging can be described by [21, 26]:

$$\delta \frac{t_2}{L_{DC}} + \frac{t_2}{L_{PD}} = 1 \quad (3)$$

where  $L_{DC}$  and  $L_{PD}$  are life under DC and life under partial discharges continuously active, respectively.

Knowing the life models and  $\delta$ ,  $t_1 + t_2 = L_i$ , which is insulation life when repetitive voltage transients are planned with mean inversion rate  $\lambda$ , can be calculated. If we consider that  $t_{2i}$  is a parameter describing the mean time at which PD are active at each voltage transient, it is possible to approximate  $\delta = t_1 / (t_{2i}\lambda)$ . Time  $t_{2i}$  could be estimated as described in [16], that is, through charging current measurements or the knowledge of permittivity and conductivity (at operating field and temperature) of the insulating material [3, 16], but a more precise estimation would require additional information regarding inception and residual fields in defects, at operating conditions [27]. In the following simulations we take values of  $t_{2i}$  in a broad range, from very short time of tens of second, which are those at which PD have highest repetition rate during transients (as mentioned above) to much longer times (hundreds and thousands second) where PD can active with significant mean repetition rate and magnitude as a result, e.g. of  $PDIV_{AC}$  much smaller than  $PDIV_{DC}$  and both lower than peak nominal voltage.

The life law can be described by the inverse power model, generally used for life and aging rate under electrical stress [28, 29]:

$$L_{DC} = t_{0,DC} \left( \frac{E}{ES_{0,DC}} \right)^{-n_{DC}} \quad (4)$$

being  $L_{DC}$  life,  $ES_{0,DC}$  the reference electric stress (generally close to the electric strength) and  $t_{0,DC}$  the relevant failure time at applied field  $E = ES_{0,DC}$ , while  $n_{DC}$  is the voltage endurance coefficient. Eq. (4) provides a straight life line in log-log coordinate system ( $\log(E)$  vs  $\log(L_{DC})$ ). Values of  $n$  for a typical HV cable insulation for DC application can range

between 15 and 20 at the operating temperature, while for AC  $n$  is slightly lower (e.g. between 10 and 15) due to the higher aging rate (that has the contribution of electro-mechanical fatigue and dielectric losses in AC with respect to DC [30, 31]. If PD are active during operating life,  $n$  drops down considerably both in AC and in DC, to values in the range 5 to 10, see Fig. 12. It can be speculated that  $n$  is the same for PD life in DC and AC, being the aging rate largely associated with PD and having roughly the same PD mechanism in DC and AC: indeed, only repetition rate changes significantly, thus the life line scale factor, not the slope (this assumption implies that life under PD is disjointed from life without PD, which is not necessarily an accurate approximation). Hence, Eq. (4) can be rewritten, in the presence of PD, as:

$$L_{PD} = t_{0,PD} \left( \frac{E}{ES_{0,PD}} \right)^{-n_{PD}} \quad (5)$$

What differs in the life model under PD (eq. (5)) from AC to DC is, therefore, the scale parameter, i.e. ( $ES_{0,PD}$ ,  $t_{0,PD}$ ) being larger in DC than in AC, Fig. 12. The scale parameter is lower when PD are present than when PD are absent.

Noting that DC aging can occur with or without PD in steady state, Eq. (3) can be then written as:

$$\delta \frac{t_2}{t_{0,DC} \left( \frac{E}{ES_{0,DC}} \right)^{-n_{DC}}} + \frac{t_2}{t_{0,PD,AC} \left( \frac{E}{ES_{0,PD,AC}} \right)^{-n_{PD}}} = 1 \quad (6)$$

when PD do not occur during life in steady state DC, and:

$$\delta \frac{t_2}{t_{0,PD,DC} \left( \frac{E}{ES_{0,PD,DC}} \right)^{-n_{PD}}} + \frac{t_2}{t_{0,PD,AC} \left( \frac{E}{ES_{0,PD,AC}} \right)^{-n_{PD}}} = 1 \quad (7)$$

when PD occur permanently during steady-state DC operation.

The parameters of (6) and (7) can be estimated by accelerated life tests carried out in order to simulate real operating conditions, thus under DC steady-state field, with or without PD and in AC with PD to account for voltage/field transients.

Eqs. (6) and (7) can be used then to exploit (3) and calculate  $L_i$ , for selected mean values of  $\lambda$ . Examples are shown in Figs. 13 to 14 15, where life estimates at design field, calculated by (6) and (7), respectively, are reported for different values of  $\lambda$ . Values of  $ES_{0,AC}$ ,  $ES_{0,DC}$ ,  $ES_{0,PD,DC}$  and  $ES_{0,PD,AC}$  are 80 kV/mm, 110 kV/mm, 105 kV/mm and 70 kV/mm, respectively, those of  $t_{0,AC}$ ,  $t_{0,DC}$ ,  $t_{0,PD,DC}$  and  $t_{0,PD,AC}$  are 20, 50, 40 and 10 second, respectively. The slopes of the life lines are  $n_{DC} = 18$ ,  $n_{AC} = 15$  and  $n_{PD} = 12$  (under the assumption, to be experimentally verified, that the activation energy of the degradation process under PD

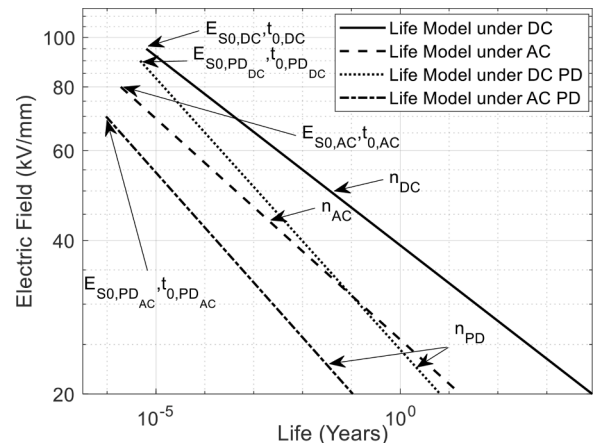
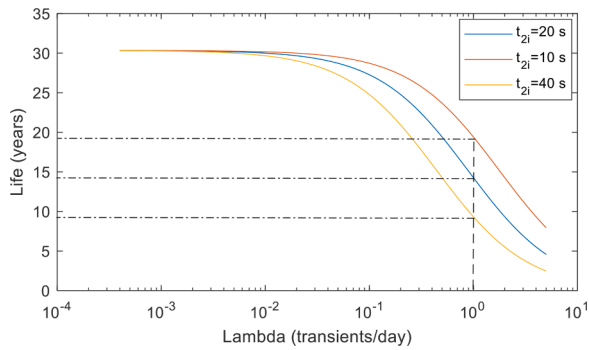
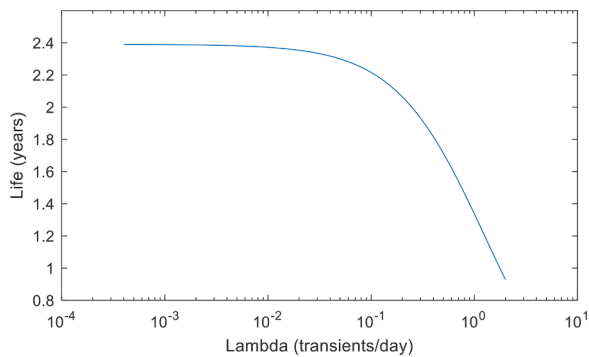


Fig. 12. Example of electrical life lines for an insulation system supplied in AC or DC, with and without PD Eqs. (4), ((5)). The rationale behind the chosen parameter values is described in the text.



**Fig. 13.** Example of electrical life behavior for an insulation system supplied in DC, without PD in steady state operation and considering mean values of  $t_{2i} = 20$  s, 10 s and 40 s, as a function of the mean rate of transients (voltage polarity inversions), from Eq. (6).



**Fig. 14.** Example of electrical life behavior for an insulation system supplied in DC, with PD in steady state operation, as a function of the mean rate of transients (voltage polarity inversions), from Eq. (7).

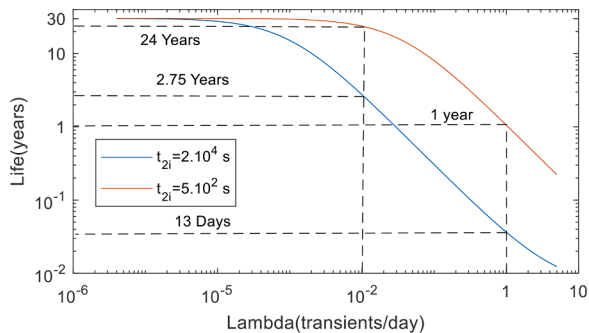


**Fig. 15.** Example of electrical life behavior for an insulation system supplied in DC, without PD in steady state operation and considering mean values of  $t_{2i} = 2.10^4$  s and  $5.10^2$  s, as a function of the mean voltage transient rate, from Eq. (6).

DC is the same as under PD AC). The design life was considered to be 30 years at 32 kV/mm design voltage without PD during operation.

As can be seen, even considering a very low mean value of the time at which PD occur at each voltage transient, e.g.  $t_{2i} = 20$  s, if voltage transient rate becomes significant, e.g. in the order of 1/day, life can be halved from 30 years to less than 15 years. If the duration through which PD lasts during each transient is halved or doubled ( $t_{2i} = 10$  s and  $t_{2i} = 40$  s respectively depending on the material), the same inversion rate of 1/day could reduce the life to less than 20 years and 10 years respectively. This is even more cumbersome when DC PD are active during operation life: even without inversion, life has a non-negligible reduction (due to the lower value of voltage endurance coefficient), which

becomes more significant upon increasing voltage transient rate.

The situation would worsen considerably when, depending on material characteristics and insulation temperature, a much higher mean value of  $t_{2i}$  is taken, as shown in Fig. 15 (this can occur e.g. when  $PDIV_{AC}$  is much smaller than  $PDIV_{DC}$  and the nominal supply voltage peak). Taking, as an example a mean value of  $t_{2i} = 2.10^4$  s, i.e.  $t_{2i} = 0.5 * \tau$  from the experiments described above at room temperature, providing  $\tau = 4.10^4$  s, if voltage transient rate becomes significant, e.g. in the order of 1/day, life can decrease dramatically, from 30 years to less than 1 month. Even with a transient rate of 0.01/day, the life would drop to 2.75 years. Increasing temperature, that is, load, conductivity can vary of at least an order of magnitude, thus e.g.  $\tau = 10^3$  s. In this case,  $t_{2i} = 0.5 * \tau = 5.10^2$  s and the curve of Fig. 15 indicates an estimated life reduction from 30 years to 1 year at a voltage transient rate of 1/day, that is, still a significant effect to be taken into account at the design stage. However, life is much closer to the design value of 30 years with respect to the previous case when the rate is 0.01/day.

This example makes clear that the design must be based on a dynamic model which account not only for electrical transients, but also for load cycling, which will be the subject of a next work.

## 7. Conclusions

Quality control, commissioning and operation of DC cable systems (and, in general, electrical apparatus) require PD testing and monitoring technologies that are effective in rejecting noise and identifying partial discharges and their sources, both under DC and AC power supply. Such technologies have not been available yet for DC supply, but this paper presents a track towards their feasibility. In particular, feasibility comes together with algorithms able potentially to separate, recognize and identify partial discharges, thus reject noise and carry out proper diagnostics, in an automatic and unsupervised manner.

The most striking consequence of being able to detect partial discharges in DC apparatus, during both steady state and voltage transients, and to understand the phenomenology behind, is the potential of evaluating aging acceleration brought about by voltage transients, which are becoming more and more frequent in modern electrical assets and grids. This is the reason of the effort made here to conceive a model that correlates allowable rate of voltage transients and specified insulation life, in the presence or partial absence of partial discharges. Developing further and validating this model on field is fundamental to achieved reliable design and operation of a DC insulation system.

## CRedit authorship contribution statement

**R. Ghosh:** Investigation, Visualization, Software, Formal analysis, Writing – review & editing. **P. Serri:** Methodology, Investigation, Resources, Writing – review & editing. **G.C. Montanari:** Conceptualization, Validation, Supervision, Writing – original draft.

## Declaration of Competing Interest

The authors declare that they have no known competing financial interests or personal relationships that could have appeared to influence the work reported in this paper.

## References

- [1] F. Kreuger, *Industrial High DC Voltage*, Delft University press, 1995.
- [2] G.C. Montanari, A contribution to unravel the mysteries of electrical aging under DC electrical stress: where we are and where we need to go, in: *Proceedings of the IEEE International Conference on Dielectrics*, 2018, pp. 1–11.
- [3] P. Serri, H. Naderiallaf, R. Ghosh, G.C. Montanari, An approach to noise rejection and partial discharge separation in DC cable testing, during steady state and voltage polarity inversion transients, *IEEE Cond. Monitor. Diagn.*, (2020), pp. 1–4.
- [4] C.K. Eoll, Theory of stress distribution in insulation of high voltage d.c. cables. Part I, *IEEE Trans. Electr. Insul.* EI-10 (2) (1975) 27–35.

- [5] G.C. Montanari, P. Seri, R. Ghosh, DC voltage supply in T&D: what about electrical insulation reliability and maintenance?, in: Proceedings of the IEEE Power and Energy Society T&D Conference, 2020, pp. 1–5.
- [6] G.C. Montanari, P. Seri, R. Ghosh, L. Cirioni, Noise rejection and partial discharge source identification in insulation system under DC voltage supply, *IEEE Trans. Dielectr. Electr. Insul.* 26 (6) (2019) 1894–1902.
- [7] P. Seri, R. Ghosh, H. Naderiallaf, L. Cirioni, G.C. Montanari, Partial discharge measurements of DC insulation systems: the influence of the energization transient, in: Proceedings of the IEEE Conference on Electric Insulators and Dielectric Phenomena, 2019, pp. 1–4.
- [8] A. Cavallini, A. Contin, G.C. Montanari, F. Puletti, Advanced PD inference in on-field measurements. I. Noise rejection, *IEEE Trans. Dielectr. Electr. Insul.* 10 (2) (2003) 216–224.
- [9] A. Cavallini, M. Conti, A. Contin, G.C. Montanari, Advanced PD inference in on-field measurements. II. Identification of defects in solid insulation, *IEEE Trans. Dielectr. Electr. Insul.* 10 (3) (2003) 528–538.
- [10] A. Contin, A. Cavallini, G.C. Montanari, G. Pasini, F. Puletti, Digital detection and fuzzy classification of partial discharge signal, *IEEE Trans. Dielectr. Electr. Insul.* 9 (3) (2002) 335–348.
- [11] R. Ghosh, P. Seri, G.C. Montanari, A track towards unsupervised partial discharge inference in electrical insulation systems, in: Proceedings of the IEEE Electric Insulator Conference, 2020, pp. 1–4.
- [12] L.A. Dissado, J.C. Fothergill, *Electrical Degradation and Breakdown in Polymers*, Peregrinus press, 1992. P.
- [13] M. Marzinotto, G. Mazzanti, The statistical enlargement law for HVDC cable lines. Part 1: theory and application to enlargement in length, *IEEE Trans. Dielectr. Electr. Insul.* 22 (1) (2015) 192–201.
- [14] M.J.P. Jeroense, P.H.F. Morshuis, Electric fields in HVDC paper-insulated cables, *IEEE Trans. Dielectr. Electr. Insul.* 5 (2) (1998) 225–236.
- [15] G. Mazzanti, M. Marzinotto, *Extruded Cables for High-Voltage Direct-Current Transmission: Advances in Research and Development*, 93, John Wiley & Sons, 2013.
- [16] E. Occhini, G. Maschio, Electrical Characteristics of Oil-Impregnated Paper as Insulation for HV DC Cables, *IEEE Trans. Power Appar. Syst.* PAS-86 (3) (1967) 312–326.
- [17] G. Mazzanti, Including the calculation of transient electric field in the life estimation of HVDC cables subjected to load cycles, *IEEE Electr. Insul. Mag.* 34 (3) (2018) 27–37.
- [18] L. Niemeyer, A generalized approach to partial discharge modeling, *IEEE Trans. Dielectr. Electr. Insul.* 2 (4) (1995) 510–528.
- [19] G.C. Montanari, R. Hebner, P. Seri, H. Naderiallaf, Partial discharge inception voltage and magnitude in polymeric cables under AC and DC voltage supply, *Jicable*, (2019), pp. 1–4.
- [20] G.C. Montanari, P. Seri, S. Franchi Bononi, M. Albertini, Partial discharge behavior and accelerated aging upon repetitive DC cable energization and voltage supply polarity inversion, *IEEE Trans. Power Deliv.* 35 (5) (2020) 1–8.
- [21] G.C. Montanari, P. Seri, P. Morshuis, R. Hebner, An approach to insulation condition monitoring and life assessment in emerging electrical environments, *IEEE Trans. Power Deliv.* 34 (4) (2019) 1357–1364.
- [22] R. Ghosh, B. Chatterjee, S. Dalai, A Method for the localization of Partial Discharge sources using Partial Discharge Pulse information from acoustic emissions, *IEEE Trans. Dielectr. Electr. Insul.* 24 (1) (2017) 237–245.
- [23] M. Cacciari, A. Contin, G.C. Montanari, Use of a mixed-Weibull distribution for the identification of partial discharge phenomena, *IEEE Trans. Dielectr. Electr. Insul.* 2 (6) (1995) 1166–1179.
- [25] G.C. Montanari, R. Hebner, P. Seri., A new algorithm to define a health index for HV and MV polymeric cables, *Jicable*, (2019), pp. 1–4.
- [26] M.A. Miner, Cumulative damage in fatigue, *J. Appl. Mech.* 12 (1945) 159–164.
- [27] G.C. Montanari, D. Fabiani, F. Ciani, Partial discharge and aging of AC cable systems under repetitive voltage transient supply, in: Proceedings of the IEEE Electric Insulator Conference, 2016, pp. 379–382.
- [28] IEC 62539, *Guide for the statistical analysis of electrical insulation breakdown data*, 2007.
- [29] G.C. Montanari, Notes on theoretical and practical aspects of polymeric insulation aging, *IEEE Electr. Insul. Mag.* 29 (4) (2013) 30–40.
- [30] G. Mazzanti, G.C. Montanari, L. Dissado, A space-charge life model for the ac electrical ageing of polymers, *IEEE Trans. Dielectr. Electr. Insul.* 6 (6) (1999) 864–875.
- [31] G.C. Montanari, P. Seri, L.A. Dissado, Aging mechanisms of polymeric materials under DC electrical stress: a new approach and similarities with mechanical aging, *IEEE Trans. Dielectr. Electr. Insul.* 26 (2) (2019) 634–641.